Journal of Photochemistry and Photobiology A: Chemistry 215 (2010) 69–75

Contents lists available at ScienceDirect

Journal of Photochemistry and Photobiology A: Chemistry

journal homepage: www.elsevier.com/locate/jphotochem

Synthesis and optical properties of two new PPV derivatives embedded on the surface of PbS nanocrystals

Piotr Piatkowski*, Wojciech Gadomski, Pawel Przybylski, Bożena Ratajska-Gadomska

Laboratory of Physicochemistry of Dielectrics and Magnetics, Department of Chemistry, University of Warsaw, ul. Zwirki i Wigury 101, 02-089 Warsaw, Poland

ARTICLE INFO

Article history:
Received 15 April 2010
Received in revised form 13 July 2010
Accepted 20 July 2010
Available online 30 July 2010

ABSTRACT

In this work we present the optical characteristics of three PPV derivatives, pure and conjugated with PbS nanocrystals (NCs). Our results exhibit strong dependence of the fluorescence lifetime of the polymers on the PbS concentration. It appears that the fluorescence lifetimes increase with the PbS NCs concentration. This is a surprising result because the presence of the quantum dots, which create new nonradiative pathways, should cause a shortening of the exciton lifetime. The observed phenomenon indicates that the surface of the PbS NCs strongly affects the excited polymer, leading to the stabilization of the emerging exciton.

1. Introduction

In this paper we present the results of our study on the complexes of conductive polymers linked to PbS quantum dots. Nowadays conductive polymers are the subject of intense research by many authors [1–10], because these materials couple the electrical and optical properties of traditional semiconductors with mechanical advantages of polymers [1]. Conjugated polymers are used as thin films or fibers as well as organic solutions. The production of polymer mixtures with various materials is a simple method for the creation of the composite materials for light processing [2–5]. These materials are attractive due to their potential applications in low-cost electronic and optoelectronic devices (LEDs, photovoltaic cells, sensors) working at lower currents and higher temperatures [6,7].

A great attention is being paid to the polymer–nanoparticle hybrid materials, especially to the materials including nanoparticles having specific spectral properties in infrared region [7,8]. Sensitizing conjugated polymers with infrared-active nanocrystal quantum dots provides a spectrally tunable means providing access to the infrared, while maintaining the advantageous properties of polymers [7]. In the last few years a lot of research groups examined photovoltaic properties of hybrid composites consisting of PbS nanocrystals (PbS NCs) and conductive polymers [7–9]. Especially poly[2-methoxy-5-(2′-ethyl-hexyloxy)-1,4-phenylenevinylene] (MEH-PPV) attracted the attention [7–9] due to its low ionization potential laying close to the ionization potential of PbS QDs. This property is critical for achieving charge separation between the nanocrystal and the polymer [7].

Composite materials including PbS QDs have better electrooptical properties than organic solar cells working in the visible spectral region and achieving 6.5% solar conversion efficiency [10]. It is possible to obtain solar cells achieving 40% conversion efficiency [4,11] in the infrared region for QD-conductive polymer hybrid materials. The light conversion efficiency of composite depends on the interactions between polymer and nanocrystals, which in turn depend on the distance, type and strength of bonds between the ingredients. These factors influence also the structure of polymers, interaction between polymer chains and optical properties of the composite, so that changes in the optical properties are the measure of interactions in hybrid material.

Measurements of luminescence in conductive polymers and conductive polymer–nanocrystal composites are important for understanding the nature of their excited states, which are responsible for the operation of electroluminescent devices [12,13]. The photo-excitation leads to generation of exciton, which then decays by radiative or nonradiative pathways. The rates of radiative and nonradiative deactivation of the excited state determine the quantum efficiency of fluorescence and the fluorescence lifetime. The longer is the lifetime of the exciton, the longer is the distance it can cover before relaxation and, thus, the possibility of polymer-quantum dot charge transfer is higher.

The modification of conjugated polymers through the side chains gives a chance to obtain more complex composite materials with, for instance, semiconductor nanocrystals. The functional groups of the lateral chains ensure better and stronger contact with the surface of nanocrystals. Polar functional groups cause the conjugated polymer to be more compatible with quantum dots. The length of the side chain, which separates the polymer from

* Corresponding author. Tel.: +48 22 8223032; fax: +48 22 8225996.
E-mail addresses: piatekpiatek@wp.pl, piatek@chem.uw.edu.pl (P. Piatkowski).

1010-6030/$ – see front matter © 2010 Elsevier B.V. All rights reserved.
doi:10.1016/j.jphotochem.2010.07.022

the nanocrystal, can modify the strengths of interactions between components of the composite material. We can expect that optical properties of the polymers depend on the lengths of the side chains separating the main polymer chain from quantum dots.

The aim of our study on optical properties of three poly(p-phenylenevinylene) (PPV) derivatives covering PbS QDs is to establish the relation between the polymer structure and the range of the mutual polymer–nanocrystal coupling. The promising results obtained for the MEH-PPV has stimulated us to look for modified PPV with shorter lateral chains, which are responsible for the reduction of the distance between the main polymer chain and the quantum dot. Thus, the ends of the chains have been modified with carboxylic group to obtain stronger interaction between PbS QDs and polymer. It is shown below that this interaction significantly influences optical properties of the polymer, especially the fluorescence lifetime.

2. Experimental

2.1. The polymer synthesis

The first polymer MEH-PPV has been obtained using a method described in [14]. Next two polymers poly[2-methoxy-5-(2′-carboxyethoxy)-1,4-phenylenevinylene] (MCE-PPV), poly[2-methoxy-5-(4′-carboxybuthoxy)-1,4-phenylenevinylene] (MCB-PPV) have been synthesized for the first time according to the modified method [14]. The three-step synthesis of the MCB-PPV and MCE-PPV is shortly outlined in Fig. 1. The compounds (**2,3**) containing alkyl chains of different lengths were obtained by the Williamson reaction between commercially available 4-methoxyphenol and appropriate bromo carboxylic acid derivatives. The key-step of the synthesis is the polymerization, at room temperature, catalyzed by potassium *tert*-butoxide to build up final compounds (**6,7**).

First, the reactions of 4-methoxyphenol (**1**) with 3-bromopropionic acid or 5-bromopentanoic acid in acetone have been carried out in the presence of potassium carbonate and potassium iodide. The mixture has been heated under reflux for 6 h. Next, the resulted 3-(4-methoxyphenyl)propanoic acid (**2**) or 5-(4-methoxyphenoxy)pentanoic acid (**3**) has been extracted with water and chloroform.

The reactants **(2)** or **(3)** received in the first step, paraformaldehyde, acetic acid and 33% HBr in acetic acid (100 ml) have been mixed and heated to 70 °C for 4 h at established N_2 atmosphere. The reaction product, 3-[2,5-bis(bromomethyl)-4-methoxyphenoxy] propanoic acid (**4**) and 5-[2,5-bis(bromomethyl)-4-methoxyphenoxy]pentanoic acid (**5**), has been diluted with chloroform followed by extraction with water and $NaHCO_3$. After that the chloroform has been removed under the reduced pressure.

The last step depends on the polymerization of (**4**) or (**5**) with potassium *tert*-butoxide in tetrahydrofuran. The reaction mixture has been stirred for 16 h. The obtained polymers have been purified by washing with ethyl acetate and dried under reduced pressure. The final polymers are presented in Fig. 2.

In order to verify the structure and purity of the synthesized materials we have performed the NMR spectra (Varian Unity Plus spectrometer operating at 700 MHz for ^{1}H NMR), using tetramethylsilane as an internal standard. The results confirm that the synthesized materials are consistent with the assumed structures without any sign of additives or impurities. Moreover, we have applied the TLC analyses performed on Merck 60 silica gel glass plate and visualized using iodine vapor, and the column chromatography carried out at atmospheric pressure using silica gel (100–200 mesh, Merck).

2.2. PbS NCs synthesis

We have synthesized PbS nanocrystals using the method described in [15]. PbO in OA (oleic acid) has been heated to obtain lead oleate precursor under nitrogen at 150 °C. After 1 h the solution was cooled to 100 °C and a solution of bis(trimethylsilyl)sulfide

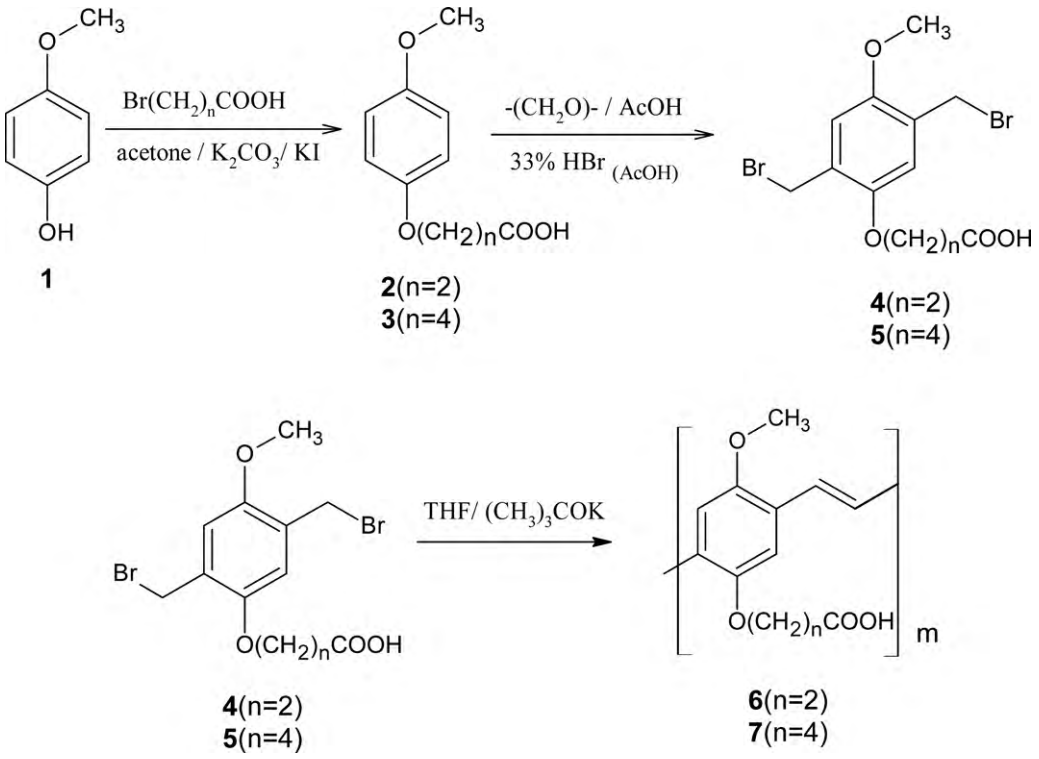

Fig. 1. Scheme of the synthesis of the polymers.

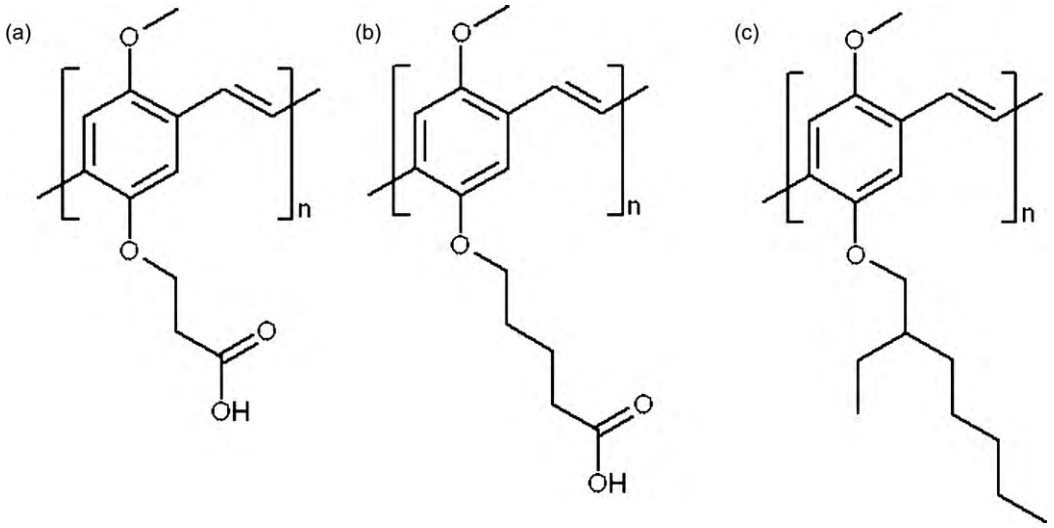

Fig. 2. (a) Poly[2-methoxy-5-(2′-carboxyethoxy)-1,4-phenylenevinylene] (MCE-PPV), (b) poly[2-methoxy-5-(4′-carboxybuthoxy)-1,4-phenylenevinylene] (MCB-PPV) and (c) poly[2-methoxy-5-(2′-ethyl-hexyloxy)-1,4-phenylenevinylene] (MEH-PPV).

TMS in octadecene was added. The resulted spherical nanocrystals were isolated from the mixture by precipitation with methanol and redispersed in chloroform. The size of spherical QDs was measured by SAXS (Small-angle X-Ray Scattering) technique and was found to be about 5 nm.

2.3. Preparing of PbS/polymer mixture

The 10^{-4} g/l solutions of three different polymers in $CHCl_3$ were prepared, then mixed with PbS NCs at the following mass ratios of polymer/PbS = 1:0.1; 1:0.2; 1:0.4; 1:0.8; 1:1.6.

2.4. Spectroscopic measurement

In order to characterize the obtained mixtures the following spectroscopic methods were used: UV–vis absorption spectroscopy (Shimadzu UV-3101PC), emission spectroscopy (FluoroLog HORIBA Jobin Yvon), time resolved emission spectroscopy (FluoroLog HORIBA Jobin Yvon with FluoroHub) and Fourier-transform IR spectroscopy (Nicolet 6700).

3. Results and discussion

3.1. IR spectroscopy

We have measured IR spectra for pure polymers, polymers mixed with PbS nanocrystals, oleic acid and PbS covered by oleic acid. The samples of polymers mixed with quantum dots were prepared as follows. First the solutions of MEH-PPV, MCE-PPV and MCB-PPV in chloroform were prepared and then the PbS NCs were added. The samples were mixed and heated at 61 °C for 5 h under nitrogen. The prepared nanocrystals were precipitated with methanol, dried and redispersed in chloroform. Next the solutions were spotted on a KBr tablets and measured by FTIR spectrometer.

Fig. 3 shows FTIR spectra of MEH-PPV (**2a**), MCE-PPV (**2b**) and MCB-PPV (**2c**) with and without PbS QDs and the spectra of oleic acid with embedded PbS nanocrystals.

There is an apparent difference between spectra of a pure oleic acid and oleic acid capping PbS quantum dots [16]. When oleic acid covers the surface of the quantum dots, the band of carboxyl at 1710 cm^{-1} in carboxyl acid and a wide OH band between 3500 and 2500 cm^{-1} disappear, whereas a band at 1544 cm^{-1}, characteristic for carboxylic acid salts, appears. This second band is characteristic

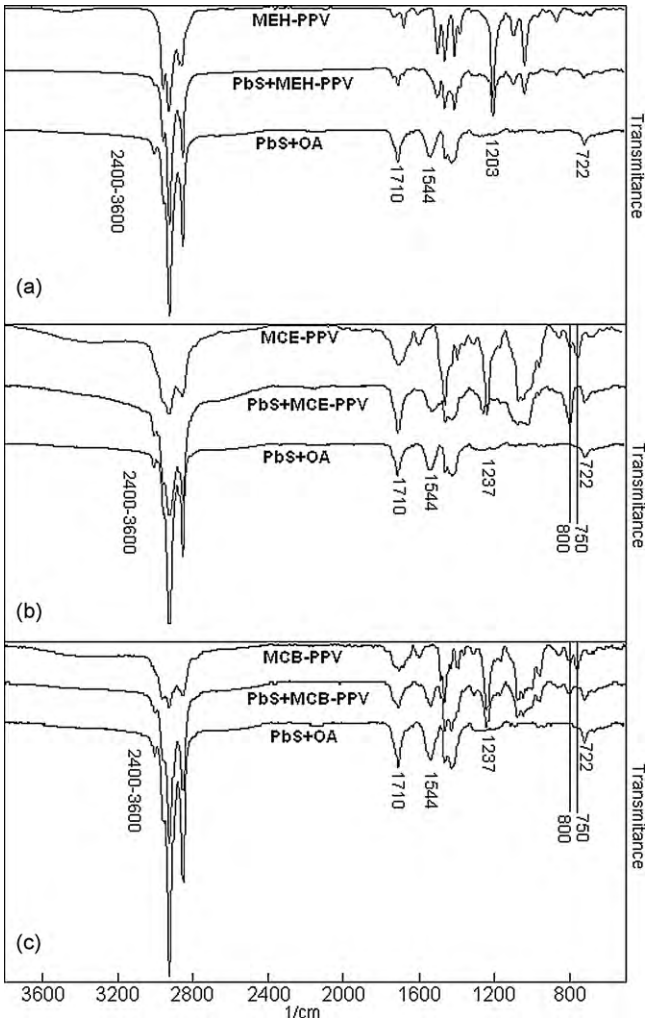

Fig. 3. FTIR spectra of: (a) MEH-PPV, (b) MCE-PPV and (c) MCB-PPV with and without PbS NCs in chloroform. All pictures contain spectra of OA covering PbS quantum dots.

for carboxylic acid salts. Oleic acid reacts with the surface of PbS nanocrystals.

As we can see in Fig. 3a–c the spectra of polymers with QDs include bands characteristic for both PPV derivatives and OA, i.e. 1710 cm^{-1} corresponding to carboxylic group of both oleic acid and polymers, 1544 cm^{-1} attributed to the COO^- group vibrations, 1464 cm^{-1} characteristic for CH_3, CH_2 bending vibrations. The band at 722 cm^{-1} corresponds to CH_2 rocking vibration in oleic acid [16]. In our case, as Fig. 2b and c shows, two bands at 760 and 800 cm^{-1} appear. These bands are attributed to the methylene rocking vibrations in the lateral chains of MCE-PPV and MCB-PPV. The polymers, which contain lateral chains with carboxylic groups, interact strongly with each other by hydrogen bonds. This is the reason why the chains of polymers are strongly bound. These mutual interactions influence the rocking vibrations of methylene groups [17,18]. In the composite with the PbS the band at 750 cm^{-1}, characteristic for both polymers, disappears, whereas the weak band at 800 cm^{-1} grows. First band can be assigned to the methylene group vibration in self-organized structure while the second band is associated with amorphous fraction of polymers. It suggests that the MCE-PPV and MCB-PPV interact with PbS, which results in destruction of their self-organized structure. The sharp bands between 2700 and 3100 cm^{-1} is characteristic for stretching vibrations of CH groups, whereas the OH groups vibrations are seen in the area 2500–3600 cm^{-1}. The wide band between 3100 and 3600 cm^{-1}, seen in Fig. 3b and c for pure polymers, is attributed to the symmetric and asymmetric modes of H-bonds created between polymer chains [19–21]. The appearance of this band proves the evidence of interchain interactions and self-organization in polymer solutions, since there are no OH groups in a single chain. In the case of MEC-PPV and MCB-PPV with embedded PbS nanocrystals the OH band becomes much weaker. It proves that the strong interactions between carboxylic groups of polymer molecules are destroyed in the presence of nanocrystals. It can be seen, in Fig. 3b and c, that at the same time the band between 2500 and 2700 cm^{-1} appears. This second band is attributed to local resonance interactions between vibrations of C–O–H and C=O groups from carboxylic group [19]. This resonance is amplified by the polymer–PbS surface interaction.

The strong band at 1202 cm^{-1} corresponds to =C–O–C– stretching vibrations in MEH-PPV [22]. As we can see in Fig. 2b and c, the similar band, located at 1237 cm^{-1}, is present in the FTIR spectrum of MCE-PPV and MCB-PPV. This band becomes significantly weaker in MCE-PPV mixed with PbS but no apparent changes can be observed for other polymers (Fig. 3a and c). Thus, we can conclude that the vibrations of =C–O–C– are probably damped by the interaction of a short lateral chain in MCE-PPV with a surface of the nanocrystal.

The presence of oleic acid peaks in the spectra of polymers with embedded nanocrystals (Fig. 3a–c) suggests that there is still OA on a surface of nanocrystals. It is possible that the band at 1544 cm^{-1} derives not only from COO^- created from OA carboxyl group but also from carboxyl groups included in the polymer lateral chains.

Fig. 3 shows that MEH-PPV covers PbS more efficiently than the next two polymers. The concentration of this polymer on the surface of the nanocrystal relative to the OA concentration is high, so that we cannot see the bands of OA in the spectra of MEH-PPV/PbS (Fig. 2a). The MCE-PPV:OA and MCB-PPV:OA concentration ratios on the surface of the PbS QDs are lower than for MEH-PPV, so that the OA bands in Fig. 3b and c are still present in a spectra of these polymers with nanocrystals.

3.2. VIS spectroscopy

We have performed the absorption and emission measurements in pure polymer solutions in chloroform. The applied polymer concentrations are low in order to reduce the influence of the interactions between polymer chains on the relaxation processes of the exciton. The absorption and emission spectra of MEH-PPV, MCE-PPV, and MCB-PPV are shown in Fig. 4. The broad absorption band resulting from PPV derivatives appears around 320–560 nm, which is due to π–π^* transitions of polyconjugated systems. Photoluminescence (PL) was excited at the wavelength 430 nm. We have fitted PL spectra with Gaussians (Fig. 3). The emission bands of these polymers consist of two bands for MCE-PPV and three bands for MEH-PPV and MCB-PPV. The distances between the components correspond to frequencies of phonon modes of polymers. We found the fitted bands to be the zero phonon line 0–0, the first 0–1 and the second 0–2 vibronic bands [23], respectively.

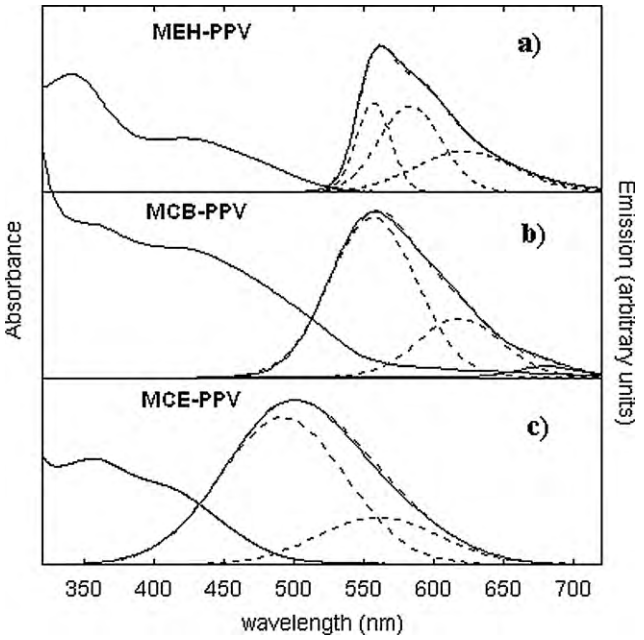

Fig. 4. Absorption and emission spectra (solid line) and Gaussians fits (dashed lines), of: (a) MEH-PPV, (b) MCE-PPV and (c) MCB-PPV in chloroform.

Optical properties of the polymers depend on the structure of the polymer chain, which influences the energy transfer between chromophores. Other authors [24] describe three ways of energy migration in polymer systems. One way depends on the electron hoping from one chromophore to another, which is typical for pendant-type polymers. Next way is the energy transfer between loops in flexible polymers. The last way is the energy migration along the polymer chain, which is characteristic for polymers consisting of carbon–carbon conjugated double bonds. We can neglect the first and the second mechanism of the energy transfer due to the structures of the polymers used in our experiments.

The absorption of light by conductive polymers causes the formation of excited states (excitons) that undergo rapid relaxation [25]. A part of excitons diffuse through the polymer, before they emit photons. Another part of excitons recombines without diffusion. When the polymer is dispersed in the solution new pathways of relaxation appear. This is due to high probability of interchain exciton delocalization. Both processes lower the coupling to the ground state and increase the radiative lifetime [25,26].

3.3. The time resolved fluorescence

The created excitons decay due to the radiative and nonradiative processes. The lifetime of each excited state τ, measured in the experiment, is expressed by both the radiative k_R and nonradiative

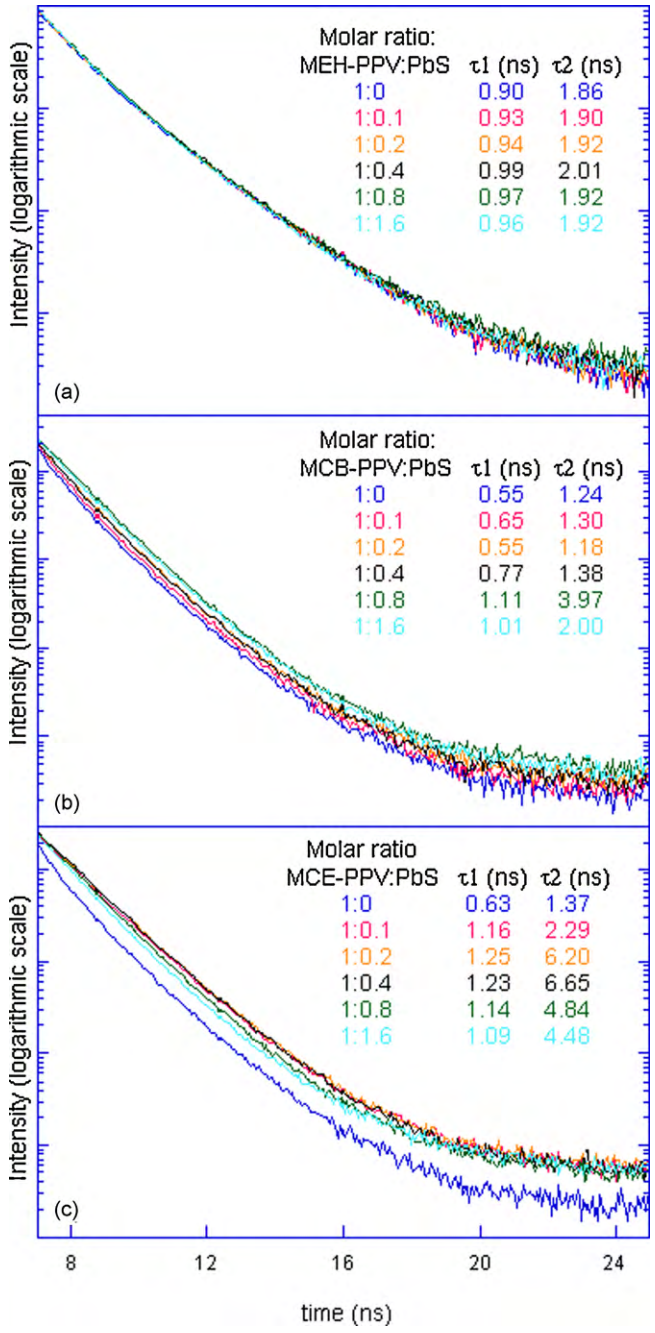

Fig. 5. Time decay curves and the measured lifetimes of the polymers excitons for different PbS NCs concentrations. The spectra contain calculated values of the lifetimes for various molar ratios of polymer to PbS. Colors of the plots correspond to the colors of the calculated values of lifetimes.

k_{NR} decay constants:

$$\frac{1}{\tau} = k_R + k_{NR} \tag{1}$$

In order to find the lifetimes of excitons, we performed the time-domain fluorescence measurements. The excitation wavelength was 440 nm, whereas the data were collected at the wavelength 500 nm for MCE-PPV and 570 nm for MEH-PPV and MCB-PPV. The results of measurements for the polymers are presented in Fig. 5. Two different time decays were observed for polymers used in the experiment. The longer lifetime of an excited state is attributed to the part of excitons, which migrate along a polymer chain before recombination [23–26]. The time decay curves in Fig. 5 have been fitted by double exponential function. It turns out that in the case of MEH-PPV the fluorescence lifetimes hardly depend on the concentration of the PbS NCs. The lifetimes shown in table in Fig. 5a have almost the same values for various concentrations of PbS. The interaction between the surface of a nanocrystal and MEH-PPV is weak, because the polymer is well separated from quantum dots with a long, unpolar chain of OA and a lateral chain of MEH-PPV. This prevents the influence of PbS on the exciton in a polymer. Fig. 5b and c shows the time decay curves for MCE-PPV and MCB-PPV and the values of lifetimes estimated for those curves. As it can be seen, the lifetimes of both polymers are strongly dependent on the concentration of PbS nanocrystals. It proves a strong interaction between quantum dots and polymers. Both lifetimes increase with the concentration of the QDs (Fig. 5b and c), but they start to decrease when the concentration of PbS QDs is too large. Probably the nonradiative pathways of deactivation become more efficient than the stabilizing effect of nanocrystals. This effect is seen for all polymers used in our experiment.

Changes of the fluorescence lifetime are much larger for MCE-PPV than for MCB-PPV. The PbS NCs influence on the fluorescence lifetime is stronger for the shorter lateral chains of the polymer, because in this case the polymer chain is closer to the surface of the PbS QDs. The increase of the time decay is attributed to more efficient charge separation in the PbS/polymer system. Then the fraction of excitons, which diffuse through the polymer chain, migrate over larger region before recombination.

3.4. Fluorescence anisotropy decay

The excitation wavelength as well as the emission wavelengths established in the fluorescence anisotropy decay experiment, for each of the polymer samples, have been the same as these used for the fluorescence decay measurements (Section 3.3). Fig. 6 shows anisotropy decays measured for all polymers and double exponential fits to the experimental data. The fits has been made according to the formula [27]:

$$r(t) = r_{01}e^{-t/\tau_{01}} + r_{02}e^{-t/\tau_{02}} \tag{2}$$

where r_{01}, r_{02} denote the zero time anisotropies and τ_{01}, τ_{02} denote decay times for the first and the second component of the anisotropy decay, respectively. The values of r_{01}, r_{02}, τ_{01}, τ_{02} are presented in Table 1. As we can see r_{01} has a value close to 0.4 for all polymers, which means that both the absorption and the emission transition moments are parallel [28]. This result suggests that the same excited states take part in both processes, i.e. absorption and emission of light. The r_{02} values, which are close to −0.1 (the absorption and emission transition moments are perpendicular [28]), demonstrate that the emission of light takes place from another electronic state than the state reached by the exciton due to the primary excitation. The anisotropy decay times corresponding to τ_{01} and τ_{02} can be attributed to longer and shorter lifetimes of the fluorescence, respectively. The longer fluorescence lifetime has been assigned to this part of excitons, which migrate along the chain before recombination. Thus, the emission connected with these excitons should be depolarized with respect to the absorbed light. It is in fact observed in our experiment, as can be seen in Fig. 6. This fraction of excitons is responsible for the fluorescence

Table 1
Emission anisotropy decay parameters of the PPV derivatives obtained from a double exponential fits to the experimental data.

	τ_{01} (ns)	r_{01}	τ_{02} (ns)	r_{01}
MEH-PPV	0.34	0.36	1.11	−0.11
MCB-PPV	0.48	0.39	1.21	−0.10
MCE-PPV	0.48	0.40	1.32	−0.11

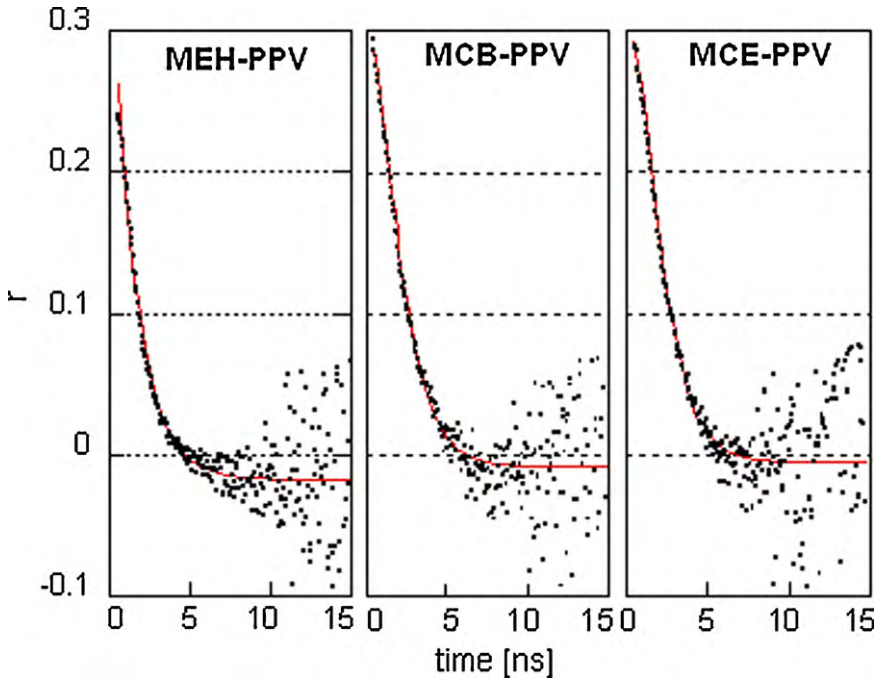

Fig. 6. Emission anisotropy decay (dots) and fitted curves (red line) of three PPV derivatives. (For interpretation of the references to colour in this figure legend, the reader is referred to the web version of the article.)

anisotropy decay described by r_{02} and τ_{02} in Eq. (2). For all polymers considered in this paper the longer anisotropy lifetimes are almost the same as the fluorescence lifetimes, whereas the shorter anisotropy decay times are significantly smaller than the corresponding fluorescence lifetimes. The existence of two components of anisotropy decay connected with two completely different values of zero time anisotropy supports our previous conclusion that two observed fluorescence lifetimes attribute to different pathways of relaxation.

4. Conclusions

For the first time we have synthesized two new derivatives of PPV, MCE-PPV and MCB-PPV and we have used it to the PbS surface passivation. The shortening of side chains reduces the distance between the main chain of the polymer and the quantum dot, while the carboxylic group of lateral chains enables the MCB-PPV and MCE-PPV to bind stronger to the surface of nanocrystal. The FTIR spectra show that the presence of quantum dots strongly affects the structure of both polymers and the interactions between polymer chains. The presence of PbS QDs destroys the hydrogen bonds between carboxylic groups of polymers, in expense of the bonds created between the polymers and the quantum dots.

Two different time decays were observed for polymers used in the experiment. The measurement of the emission anisotropy decay provides the additional proof that these decays result from different pathways of deactivation. The first transition takes place directly from the excited state and the second one is preceded by migration along the polymer chain. We have found that the lifetime of an exciton increases with the concentration of nanocrystals. It means that the charge separation is more efficient in the presence of PbS QDs and the efficiency of the nonradiative processes diminishes, see Eq. (1). Thus, we observe a significant enhancement of the survival probability of the photogenerated charges upon doping with PbS QDs. This is a surprising result since one might expect that the inclusion of QDs should create a new nonradiative pathways resulting in the exciton lifetime decrease. On the other hand creation of the nanocrystal–polymer system destroys the aggregates of polymers, thereby it can destroy the nonradiative ways of exciton deactivation, for instance interchain energy migration [25,26]. The fluorescence lifetimes strongly depend on the distance between the nanocrystal and the polymer. The shorter is the side chain of polymer the stronger is the nanocrystal influence on the exciton and the longer is fluorescence decay time. Thus, the final conclusion is that embedding quantum dots into the matrix of conducting polymers of the appropriate structure may significantly improve the efficiency of the charge transport along the polymer chain.

Acknowledgment

This work was supported by the Ministry of Scientific Research and Information Technology in 2008–2010, Project No. N N20423984.

References

[1] D. Braun, A.J. Heeger, Visible light emission from semiconducting polymer diodes, Appl. Phys. Lett. 58 (1991) 1982–1984.
[2] D. Wei, G. Amaratunga, Photoelectrochemical cell and its applications in optoelectronics, Int. J. Electrochem. Sci. 2 (2007) 897–912.
[3] S. Hinds, L. Levina, E.J.D. Klem, G. Konstantatos, V. Sukhovatkin, E.H. Sargent, Smooth-morphology ultrasensitive solution-processed photodetectors, Adv. Mater. 20 (2008) 4398–4402.
[4] G.I. Koleilat, L. Levina, H. Shukla, S.H. Myrskog, S. Hinds, A.G. Pattantyus-Abraham, E.H. Sargent, Efficient, stable infrared photovoltaics based on solution-cast colloidal quantum dots, ACS Nano 2 (2008) 833–840.
[5] J. Lee, V.C. Sundar, J.R. Heine, et al., Full color emission from II–VI semiconductor quantum dot-polymer composites, Adv. Mater. 12 (2000) 1102–1105.
[6] E.H. Sargent, Infrared quantum dots, Adv. Mater. 17 (2005) 515–522.
[7] S.A. McDonald, G. Konstantatos, S. Zhang, P.W. Cyr, E.J.D. Klem, L. Levina, E.H. Sargent, Solution-processed PbS quantum dot infrared photodetectors and photovoltaics, Nat. Mater. 4 (2005) 138–142.
[8] K.P. Fritz, S. Guenes, J. Luther, Sandeep Kumara, N. Serdar Sariciftci, G.D. Scholes, IV–VI nanocrystal–polymer solar cells, J. Photochem. Photobiol. A: Chem. 195 (2008) 39–46.
[9] S.A. McDonald, P.W. Cyr, L. Levina, E.H. Sargent, Photoconductivity from PbS-nanocrystal/semiconducting polymer composites for solution processible, quantum-size tunable infrared photodetectors, Appl. Phys. Lett. 85 (2004) 2089–2091.
[10] J.Y. Kim, K. Lee, N.E. Coates, D. Moses, T. Nguyen, M. Dante, A.J. Heeger, Efficient tandem polymer solar cells fabricated by all-solution processing, Science 317 (2007) 222–225.

[11] A. Marti, G.L. Araujo, Limiting efficiencies for photovoltaic energy conversion in multigap systems, Sol. Energy Mater. Sol. Cells 43 (1996) 203–222.
[12] S.A. Arnautov, A.E.M. Nechvolodovaa, A.A. Bakulinb, S.G. Elizarovb, A.N Khodarevb, D.S. Martyanovb, D.Yu. Paraschukb, Properties of MEH-PPV films prepared by slow solvent evaporation, Synth. Met. 147 (2004) 287–291.
[13] V.M. Burlakov, K. Kawata, H.E. Assender, G.A.D. Briggs, Discrete hopping model of exciton transport in disordered media, Phys. Rev. B 72 (1–5) (2005) 075206.
[14] C.J. Neef, J.P. Ferraris, MEH-PPV: improved synthetic procedure and molecular weight, Control Macromol. 33 (2000) 2311–2314.
[15] M.A. Hines, G.D. Scholes, Colloidal PbS nanocrystals with size-tunable near-infrared emission: observation of post-synthesis self-narrowing of the particle size distribution, Adv. Mater. 15 (2003) 1844–1849.
[16] S. Chen, W. Liu, Oleic acid capped PbS nanoparticles: synthesis, characterization and tribological properties, Mater. Chem. Phys. 98 (2006) 183–189.
[17] N. Kang, Y.-Z. Xu, J.-G. Wu, W. Feng, S.-F. Weng, D.-F. Xu, The correlation between crystalline behavior of polyethylene segments and hydrogen bonds among carboxyl groups in ethylene–acrylic acid copolymers, Phys. Chem. Chem. Phys. 2 (2000) 3627–3630.
[18] Z. Ren, D. Maa, Y. Wang, G. Zhao, Molecular structure and hydrogen bonds in solid dimethylol propionic acid (DMPA), Spectrochim. Acta Part A: Mol. Biomol. Spectrosc. 59 (2003) 2713–2722.
[19] C. Emmeluth, M.A. Suhm, David Luckhaus, A monomers-in-dimers model for carboxylic acid dimers, J. Chem. Phys. 118 (2003) 2242–2255.
[20] G.M. Florio, E.L. Sibert, T.S. Zwiera, Fluorescence-dip IR spectra of jet-cooled benzoic acid dimer in its ground and excited singlet states, Faraday Discuss. 118 (2001) 315–330.
[21] L.M. Babkov, E.S. Vedyaeva, G.A. Puchkovskaya, IR spectra, polymorphism, and intermolecular interactions in carboxylic acids, J. Struct. Chem. 42 (2001) 32–37.
[22] X. Wu, G. Shi, L. Qu, J. Zhang, F.E. Chen, Novel route to poly(*p*-phenylene vinylene) polymers, J. Polym. Sci. A 41 (2003) 449–455.
[23] Y.-Y. Lin, Ch.-W. Chen, J. Chang, T.Y. Lin, I.S. Liu, W.-F. Su, Exciton dissociation and migration in enhanced order conjugated polymer/nanoparticle hybrid materials, Nanotechnology 17 (2006) 1260–1263.
[24] J. Guillet, Polymer Photophysics and Photochemistry, Cambridge University Press, New York, 1985, ch.9.
[25] T.-Q. Nguyen, V. Doan, B.J.J. Schwartz, Conjugated polymer aggregates in solution: control of interchain interactions, J. Chem. Phys. 110 (1999) 4068–4078.
[26] A. Rassamesard, Y.-F. Huang, H.-Y. Lee, T.-S. Lim, M.C. Li, J.D. White, J.H. Hodak, T. Osotchan, K.Y. Peng, S.A. Chen, J.-H. Hsu, O.M. Hayashi, W. Fann, Environmental effect on the fluorescence lifetime and quantum yield of single extended luminescent conjugated polymers, J. Phys. Chem. C 113 (2009) 18681–18688.
[27] J.R. Lakowicz, Principles of fluorescence spectroscopy, Springer Science+Business Media, New York, 2006 (Chapter 1).
[28] R.H. Austin, S.S. Chan, T.M. Jovin, Rotational diffusion of cell surface components by time-resolved phosphorescence anisotropy, Proc. Natl. Acad. Sci. U.S.A. 76 (1979) 5650–5654.